

MOL #89482

Title Page

**The antiallergic mast cell stabilizers lodoxamide and bufrolin as the first high
and equipotent agonists of human and rat GPR35**

Amanda E. MacKenzie, Gianluigi Caltabiano, Toby C. Kent, Laura Jenkins, Jennifer
E. McCallum, Brian D. Hudson, Stuart A. Nicklin, Lindsay Fawcett, Rachel Lane,
Steven J. Charlton and Graeme Milligan

Molecular Pharmacology Group, Institute of Molecular, Cell and Systems Biology,
(AEM, GC, LJ, JEM, BDH, GM) and Institute of Cardiovascular & Medical Sciences,
(JEM, SAN) College of Medical, Veterinary and Life Sciences, University of
Glasgow, Glasgow G12 8QQ, Scotland, United Kingdom

Laboratori de Medicina Computacional, Unitat de Bioestadística,
Facultat de Medicina, Universitat Autònoma de Barcelona, 08193 Bellaterra, Spain
(GC)

Novartis Institutes for Biomedical Research, Horsham, RH12 5AB, United Kingdom
(TCK, LF, RL SJC)

MOL #89482

Running Title Page

Running title: Mast cell stabilizers and GPR35

To whom correspondence should be addressed: Graeme Milligan, Wolfson Link
Building 253, University of Glasgow, Glasgow G12 8QQ, Scotland, U.K. Tel +44
141 330 5557, FAX +44 141 330 5481, e-mail: Graeme.Milligan@glasgow.ac.uk

Manuscript information

Text Pages:	43
Tables:	3
Figures:	9
Words in Abstract:	230
Words in Introduction:	600
Words in Discussion:	1343
References	33

Nonstandard Abbreviations

BRET, bioluminescence resonance energy transfer; ECL2, extracellular loop 2;
eYFP, enhanced Yellow Fluorescent Protein; GPCR, G protein-coupled receptor;
PCA, passive cutaneous anaphylaxis; SNP, single nucleotide polymorphism; TMD,
transmembrane domain.

MOL #89482

Chemical names: amlexanox, 2-amino-7-(1-methylethyl)-5-oxo-5H-[1] benzopyrano[2,3-b]pyridine-3-carboxylic acid; BRL10833, 5,6-dimethyl-2-nitro-1H-indene-1,3(2H)-dione; bufrolin, 6-butyl-4,10-dioxo-1,7-dihydro-1,7-phenanthroline-2,8-dicarboxylic acid cromolyn disodium, disodium; 5-[3-(2-carboxylato-4-oxochromen-5-yl)oxy-2-hydroxypropoxy]-4-oxochromene-2-carboxylate; doxantrazole (3-(1H-tetrazol-5-yl)-9H-thioxanthen-9-one 10,10-dioxide monohydrate, ketitofen fumarate, 4-(1-methylpiperidin-4-ylidene)-4,9-dihydro-10H-benzo[4,5]cyclohepta[1,2-*b*]thiophen-10-one, lodoxamide, (2-[2-chloro-5-cyano-3-(oxaloamino)anilino]-2-oxoacetic acid, nedrocromil sodium, disodium; 9-ethyl-4,6-dioxo-10-propylpyrano[3,2-*g*]quinoline-2,8-dicarboxylate, pemirolast potassium, 9-methyl-3-(1H-tetrazol-5-yl)-4H-pyrido[1,2-*a*]pyrimidin-4-one, potassium salt, tranilast, 2-[[3-(3,4-dimethoxyphenyl)-1-oxo-2-propenyl]amino] benzoic acid, zaprinast, 1,4-dihydro-5-(2-propoxyphenyl)-7H-1,2,3-triazolo(4,5-*d*)pyrimidin-7-one.

MOL #89482

Abstract

Lack of high potency agonists has restricted analysis of the G protein-coupled receptor GPR35. Moreover, marked variation in potency and/or affinity of current ligands between human and rodent orthologs of GPR35 has limited their productive use in rodent models of physiology. Based on the reported modest potency of the anti-asthma and antiallergic ligands cromolyn disodium and nedocromil sodium we identified the related compounds lodoxamide and bufrolin as high potency agonists of human GPR35. Unlike previously identified high potency agonists that are highly selective for human GPR35, both lodoxamide and bufrolin displayed equivalent potency at rat GPR35. Further synthetic antiallergic ligands, either sharing features of the standard surrogate agonist zaprinast, or with lodoxamide and bufrolin, were also shown to display agonism at either human or rat GPR35. As both lodoxamide and bufrolin are symmetric di-acids their potential mode of binding was explored via mutagenesis based on swapping between the rat and human orthologs non-conserved arginine residues within proximity of a key conserved arginine at position 3.36. Computational modelling and ligand docking predicted the contributions of different arginine residues, other than at 3.36, in human GPR35 for these two ligands and was consistent with selective loss of potency of either bufrolin or lodoxamide at distinct arginine mutants. The computational models also suggested that bufrolin and lodoxamide would display reduced potency at a low frequency human GPR35 SNP. This prediction was confirmed experimentally.

MOL #89482

Introduction

Although poorly characterized, the seven transmembrane domain (TMD), G protein-coupled receptor (GPCR) GPR35 has attracted attention as a potential therapeutic target in disease areas ranging from pain to hypertension (Milligan, 2011, MacKenzie et al., 2011). Although indicated to be a receptor responsive to the endogenously produced tryptophan metabolite kynurenic acid (Wang et al., 2006), lack of convergence on this issue has resulted in a number of efforts to identify surrogate agonist ligands that might be used to help further define the roles of this receptor. Although a number of such ligands have been identified (Taniguchi et al., 2006, Jenkins et al., 2010, Zhao et al., 2010, Deng et al., 2012, Neetoo-Isseljee et al., 2013, Funke et al., 2013), many of these are either of modest potency and/or display markedly different potency at human and rodent orthologs of GPR35 (Jenkins et al., 2010, Neetoo-Isseljee et al., 2013, Funke et al., 2013). This has posed challenges both in efforts to define the orthosteric binding pocket of the receptor and to use rodents and cell lines derived from such animals to further explore the function of GPR35. It would, therefore, be of particular value to identify agonists with similar and high potency at the human and rodent orthologs of GPR35 and to better understand the basis of ligand selectivity between species. One common feature of human and rat GPR35 is the presence of an arginine residue in TMD III (position 3.36 in the Ballesteros and Weinstein (1995) residue numbering system) that when mutated to a non-basic residue results in virtual complete loss of potency of kynurenic acid and a number of GPR35 surrogate agonist ligands (Jenkins et al., 2011). Importantly, arginine 3.36 is conserved in a number of other receptors, such as the lactate receptor

MOL #89482

GPR81 (Liu et al., 2009), that are activated by endogenously generated acids, suggesting that kynurenic acid and potentially other acidic ligands, interact with this residue via an ionic interaction.

Recently it was shown that the anti-asthma and antiallergic agents cromolyn disodium (Jenkins et al., 2010, Yang et al., 2010) and nedocromil sodium (Yang et al., 2010) act as moderately potent agonists of GPR35. These ligands are both di-acids with marked mirror image symmetry (**Figure 1**). Based on this we considered if a number of other symmetric di-acids might also be GPR35 agonists. The antiallergic mast cell stabilizers lodoxamide and bufrolin both display these characteristics (**Figure 1**) and were shown to be the most potent agonists of both human and rat GPR35 yet reported. We then considered whether activation of GPR35 might provide a common mechanism of action of a broad group of mast cell stabilizers. This, however, was not the case. Zaprinast (Tanaguchi et al., 2006, Jenkins et al., 2010, 2011) has become the standard surrogate agonist of GPR35 and, akin to zaprinast, a number of mast cell stabilizers also contain an acid bioisostere. Because zaprinast is an example of a ligand that displays marked variation in potency between rodent and human GPR35 (Tanaguchi et al., 2006, Jenkins et al., 2010, 2011) this also encouraged us to also explore the contributions of a series of non-maintained arginine residues within regions of the receptor species orthologs that are predicted to define the ligand binding pocket. Cross-species alterations of such residues provided novel insights into the binding pocket. Computational modelling and ligand docking studies provided strong rationale for the experimental data and further suggested that a specific single non-synonymous polymorphism (SNP) variant in human GPR35 might

MOL #89482

show differences in ligand potency. This hypothesis was tested and shown to be valid, whereas ligand potency at other human SNP variants was unaffected.

Materials and Methods

Materials – Materials for cell culture were from Sigma-Aldrich (Gillingham, Dorset, UK), Life Technologies (Paisley, Strathclyde, UK), or PAA Laboratories Ltd (Yeovil, Somerset, UK). Polyethylenimine linear MW-25000 was from Polysciences Inc (Warrington, PA). Zaprinast, (1,4-dihydro-5-(2-propoxyphenyl)-7H-1,2,3-triazolo(4,5-d)pyrimidin-7-one) was purchased from Tocris Bioscience (Bristol, UK). Amlexanox, (2-amino-7-(1-methylethyl)-5-oxo-5H-[1]benzopyrano[2,3-b]pyridine-3-carboxylic acid), cromolyn disodium (disodium;5-[3-(2-carboxylato-4-oxochromen-5-yl)oxy-2-hydroxypropoxy]-4-oxochromene-2-carboxylate), doxantrazole (3-(1H-tetrazol-5-yl)-9H-thioxanthen-9-one 10,10-dioxide monohydrate), ketitofen fumarate 4-(1-methylpiperidin-4-ylidene)-4,9-dihydro-10H-benzo[4,5]cyclohepta[1,2-b]thiophen-10-one, pemirolast potassium (9-methyl-3-(1H-tetrazol-5-yl)-4H-pyrido[1,2-a]pyrimidin-4-one potassium salt), tranilast (2-[[3-(3,4-dimethoxyphenyl)-1-oxo-2-propenyl]amino] benzoic acid) and Hoechst 33258 were purchased from Sigma-Aldrich (Gillingham, Dorset, UK). Bufrolin, (6-butyl-4,10-dioxo-1,7-dihydro-1,7-phenanthroline-2,8-dicarboxylic acid), BRL 10833, 5,6-dimethyl-2-nitro-1H-indene-1,3(2H)-dione and nedocromil sodium (disodium;9-ethyl-4,6-dioxo-10-propylpyrano[3,2-g]quinoline-2,8-dicarboxylate) were synthesized in house. Lodoxamide (2-[2-chloro-5-cyano-3-(oxaloamino)anilino]-2-oxoacetic acid) was a gift of Dr. Ed McIver and Dr. Debra Taylor, Medical Research Council Technology,

MOL #89482

London, UK. With the exception of pemirolast potassium which was reconstituted in dH₂O, ligands were initially dissolved in DMSO and then diluted in assay buffer.

Plasmids and mutagenesis

All novel plasmids employed expressed human (GPR35a or GPR35b) or rat GPR35 receptor constructs which contain an enhanced yellow fluorescent protein (eYFP) fused to the C terminal and an N terminal FLAG epitope tag as described previously (Jenkins et al., 2010, 2011). Individual amino acid swap mutations between human and rat sequences were introduced into the FLAG-hGPR35a-eYFP or FLAG-rGPR35-eYFP constructs using the QuickChange method (Stratagene). All mutations were confirmed by DNA sequencing.

Cloning of human GPR35b

Human GPR35b, containing a FLAG epitope (amino acid sequence DYKDDDDK) at the N-terminus, was produced from cDNA generated from HT29 cell by PCR using the following primers: sense,

5'ACTCAAAGCTTGCCACCATGGATTACAAGGATGACGACGATAAGCTGAGT
GGTTCCCGGG 3', and antisense: 5'ACTCGCGGCCGCAGGCGAGGGTCACGC

3'. The *Hin*DIII and *Not*I restriction sites used for cloning are underlined. The resulting construct was cloned in-frame into the *Hin*DIII/*Not*I sites of an eYFP-pcDNA5/FRT/TO plasmid and integrity of the fusion was confirmed by DNA sequencing.

Cell culture and transfection

MOL #89482

Flp-InTM TRExTM 293 cells were maintained in Dulbecco's modification of Eagle's medium (DMEM) without sodium pyruvate (Life Technologies Inc), supplemented with 10% (v/v) fetal bovine serum, 1% penicillin/streptomycin mixture, and 10 μ g/mL blasticidin. HEK293T cells were maintained in DMEM supplemented with 0.292 g/L L-glutamine, 10% (v/v) fetal bovine serum, and 1% penicillin/streptomycin mixture. Transient transfections using HEK293T cells were performed using polyethylenimine, with experiments carried out 24h post transfection (Jenkins et al., 2011). HT-29 human adenocarcinoma cells were purchased from the American Type Culture Collection (Gaithersburg, MD) and maintained in McCoy's 5A (Modified) media containing 25 mM 4-(2-hydroxyethyl)-1-piperazineethanesulfonic acid (HEPES). PathHunterTM β -arrestin recruitment Chinese hamster ovary (CHO-K1) cells stably expressing human GPR35 and β -arrestin-2 (DiscoverX, Fremont). (Neeto-Isserjee et al., 2013) were routinely passaged in complete growth medium (DMEM/F12 with GlutaMAX + 10% fetal bovine serum). All cells were maintained at 37°C and 5% CO₂ in a humidified cell culture incubator.

GPR35- β -arrestin-2 interaction assays

Utilized two distinct methods: The PathHunterTM β -arrestin-2 recruitment assay was performed using a Chinese hamster ovary (CHO-K1) cell line stably expressing human GPR35 and β -arrestin-2 (DiscoverX, Fremont) as described previously (Neetoo-Isseljee et al., 2013). The bioluminescence resonance energy transfer (BRET)-based β -arrestin-2 recruitment assay was performed using HEK293T cells transfected transiently to co-express forms of human GPR35a, human GPR35b or rat GPR35 along with β -arrestin-2, as described by Jenkins et al., (2011).

MOL #89482

ArrayScan™ high content analysis of GPR35 internalization

FLAG-hGPR35-eYFP Flp-In™ T-REx™ 293 cells were seeded into poly-D-lysine coated black clear bottom 96 well plates at a density of 80,000 cells/well. Receptor expression was induced via the addition of doxycycline (100 ng/mL) six hours after seeding. Twenty four hours later, cells were washed twice with serum free medium and incubated with ligand for 45 min at 37°C, before being fixed with paraformaldehyde (4% v/v). Cells were washed with PBS and incubated with 10 µg/mL Hoechst nuclear stain at 37°C for 30 min to allow determination of cell number. Receptor internalization was quantified using a Cellomics ArrayScan™ II high content imager, which detected FLAG-hGPR35-eYFP receptor trafficking to endocytic recycling compartments.

Visualization of GPR35 internalization

FLAG-hGPR35-eYFP Flp-In™ T-REx™ 293 cells were cultured on poly-D-lysine coated glass coverslips and incubated for 24 h before treatment with doxycycline (100 ng/mL) to induce receptor expression. Live cells were then imaged using a Zeiss VivaTome spinning disk confocal microscopy system. Images were taken prior to the addition of ligand, and every 15 min following ligand addition for a total of 45 min.

Epic® label free Dynamic Mass Redistribution assays

HT-29 cells were plated in complete medium at a density of 30,000 cells/well into fibronectin coated Epic® 384 well plates (Corning), at a volume of 50 µL/well, prior to incubation for 24 h at 37°C in a humidified atmosphere containing 5% CO₂. At

MOL #89482

95% confluence, the cells were washed three times with serum free medium containing 25mM HEPES using a Biomek[®] FXP automated liquid handling system, before a final addition of serum free medium containing 0.01% DMSO. Cells were then equilibrated for 90 min at 26°C in the Epic[®] BT system (Corning), before acquisition of basal data for 2 min. Ligand, prepared in serum free medium and normalized for DMSO concentration (0.01%), was then added using the Biomek[®] FXP at a volume of 10 μ L/well before measurement of dynamic mass redistribution (DMR) for 60 min at 26°C. Kinetic reads generated using the whole cell scanning application (four reads/well) were baseline corrected, and concentration-response curves plotted from data generated five minutes post ligand addition using GraphPad Prism software. Antagonist assays were performed as described for the agonist format, except that the antagonist was added for 30 min prior to the addition of agonist, with the agonist response plotted from data generated at 35 min. Data represent n = 3 and were performed in quadruplicate.

ELISA assay

PathHunter[™] CHO-K1 cells stably expressing human GPR35 and β -arrestin-2 (DiscoverRx, Fremont) were seeded into clear 96 well plates at a density of 30,000 cells/well in complete growth medium. Receptor expression was induced via the addition of doxycycline (100 ng/mL). Twenty four hours later, cells were washed with wash buffer (PBS with 1% BSA) and incubated with a 1:300 dilution of anti-FLAG antibody (Sigma-Aldrich, Gillingham, Dorset, UK) in complete growth medium for 120 min at 37°C. Medium only controls were also run. Cells were washed with wash buffer and incubated with a 1:1000 dilution of anti-mouse HRP (Cell

MOL #89482

Signaling Technology, Danvers, MA) in complete growth medium at 37°C for 40 min. Cells were washed with wash buffer and incubated with ABTS substrate (Peprotech, London, UK) for 40 min at room temperature. The plate was centrifuged at 3000 rpm, 40µL of supernatant transferred to a clear 96-well plate and the plate read on Synergy Platereader (Biotek, Pottom, Bedfordshire, UK) at 405nm and 605nm. 605nm values were subtracted from 405nm values. Mean values for medium only controls were subtracted from anti-FLAG values and the resulting values divided by the mean wild-type value to give expression relative to wild-type.

Computational methods

Modeller 9v8 (Martí-Renom et al., 2000) was used to model the TMD helices I-VII, and both intracellular and extracellular loops 1-3, of human and rat GPR35 using the structure of the protease-activated receptor 1 as template (PDB code 3VW7) (Zhang et al., 2012). Ligands were docked, by interactive computer graphics, into the receptor models with a negatively charged group interacting with Arg3.36. These ligand-receptor complexes were embedded in membrane bilayer and refined by energy minimization and molecular dynamics simulations with gromacs4.6 (Hess et al., 2008) using a previously described protocol (Cordomí et al., 2012). Modelling figures were generated using Pymol 1.5.3. (Schrodinger, 2012).

Data analysis

All data presented represent mean \pm standard error of at least three independent experiments. Data analysis and curve fitting was carried out using Graphpad Prism software package v5.0. Concentration-response data were plotted on a log axis, where

MOL #89482

the untreated vehicle control condition was plotted at one log unit lower than the lowest test concentration of ligand and fitted to three-parameter was performed using standard approaches. Statistical analysis was carried out using 1-way analysis of variance followed by Dunnett's post-hoc test.

Results

Previous studies have shown that the anti-asthma and antiallergic agents cromolyn disodium (Jenkins et al., 2010, Yang et al., 2010) and nedocromil sodium (Yang et al., 2010) are modestly potent agonists of GPR35. This was confirmed in a PathHunter™ human GPR35a-β-arrestin-2 interaction and complementation assay (**Table 1**) with nedocromil sodium ($EC_{50} = 0.97 \pm 0.09 \mu\text{M}$) being some 3 fold some potent than cromolyn disodium ($EC_{50} = 2.98 \pm 1.27 \mu\text{M}$). As GPR35 is expressed by human mast cells and levels are reportedly upregulated by exposure to the allergic stimulus IgE (Yang et al., 2010), we set out to investigate whether other antiallergic ligands and mast cell stabilizers might also act as agonists at GPR35 and, if so, potentially provide a common mode of action. Bufrolin (also designated ICI 74917) (**Figure 1**), a compound shown originally to be an effective inhibitor of passive cutaneous anaphylaxis (PCA) in rats, a model of IgE-induced allergy, was a highly potent agonist of human GPR35a ($EC_{50} = 2.9 \pm 0.7 \text{ nM}$) (**Table 1**), whilst another anti-allergic compound effective in the PCA model, sodium nivalmedone (BRL 10833) (Lumb et al., 1979) although substantially less potent ($EC_{50} = 1.9 \pm 0.3 \mu\text{M}$) also displayed agonism at human GPR35a (**Table 1**). Interestingly, lodoxamide (**Figure 1**), used topically for the treatment of allergic conjunctivitis, was also

MOL #89482

identified as a highly potent ($EC_{50} = 1.6 \pm 0.4$ nM) agonist of GPR35a. Despite this overlap of GPR35 agonism and either clinical use or initial development as anti-asthma or antiallergic medicines this did not, however, provide a common mode of action of mast cell stabilizing compounds. For example, ligands such as tranilast, which has been used to treat allergic disorders such as asthma, allergic rhinitis and atopic dermatitis, displayed no agonist activity (**Table 1**).

To build on these initial studies we also utilized a distinct human GPR35a- β -arrestin-2 interaction assay that is based on agonist-induced bioluminescence resonance energy transfer (BRET) (Jenkins et al., 2010, 2011, 2012). Although, as noted previously (Neeto-Isserjee et al., 2013), whilst this assay often displays slightly lower sensitivity than the PathHunter™ protein complementation assay described above, both lodoxamide ($EC_{50} = 3.6 \pm 0.2$ nM) and bufrolin ($EC_{50} = 12.8 \pm 0.7$ nM) were again highly potent human GPR35a agonists (**Figure 2A**), displaying some 200-700 fold greater potency than the current standard surrogate ligand, zaprinast ($EC_{50} = 2.6 \pm 0.1$ μ M) (**Figure 2A**). Moreover, tranilast was again inactive in this assay format (**data not shown**), as were two further mast cell stabilizers, pemirolast (**Figure 2A**) and ketotifen fumarate (**data not shown**). Furthermore, doxantrazole, another ligand trialled for the treatment of asthma, although displaying modest potency ($EC_{50} = 3.4 \pm 0.5$ μ M), was clearly a partial agonist (**Figure 2A**), as was amlexanox ($EC_{50} = 4.1 \pm 0.5$ μ M) (**Figure 2A**), recently also described (Neeto-Isserjee et al., 2013, Southern et al., 2013) as a GPR35 agonist.

Although the above studies clearly demonstrated that GPR35a is activated by a number of antiallergic ligands, they did not suggest that this GPCR might provide a

MOL #89482

common target and mechanism of action for the broad class of ligands. However, human GPR35 exists as two distinct splice variant forms, whereby GPR35b differs from GPR35a by the presence of an additional 31 amino acids inserted into the extreme N-terminal, extracellular domain (Okumura et al., 2004, Milligan, 2011). To assess any potentially relevant differences in ligand pharmacology between these variants we cloned GPR35b from human HT-29 colorectal adenocarcinoma cells and following in-frame addition of eYFP to the C-terminal tail of the receptor and introduction of a N-terminal FLAG-epitope tag sequence to mimic the GPR35a construct, BRET-based GPR35b- β -arrestin-2 interaction assays were also performed in HEK293T cells. Although the absolute signal in these assays was substantially lower than when using GPR35a, the overall results and the measured potency and rank order of ligands including lodoxamide, bufrolin, zaprinast and cromolyn disodium were indistinguishable from GPR35a (**Figure 2B**), whilst both amlexanox and doxantrazole remained partial agonists (**Figure 2B**).

A number of previously reported GPR35 agonists cause rapid and extensive internalization of the receptor (Jenkins et al., 2011). We, therefore, used this as a further endpoint to determine potential effects of these compounds on human GPR35a. Flp-InTM T-RexTM 293 cells stably harboring human FLAG-GPR35a-eYFP at the Flp-InTM T-RExTM locus were induced to express the receptor by addition of the antibiotic doxycycline (Jenkins et al., 2011). Using high content analysis of the cellular distribution of eYFP, the effect and high potency of lodoxamide ($EC_{50} = 5.4 \pm 0.6$ nM) and bufrolin ($EC_{50} = 22.7 \pm 2.0$ nM) as GPR35a agonists was confirmed (**Figure 3**). Moreover, as in the β -arrestin-2 interaction assay these two compounds

MOL #89482

were substantially more potent than either zaprinast ($EC_{50} = 4.1 \pm 1.0 \mu\text{M}$) or cromolyn disodium ($EC_{50} = 3.7 \pm 1.2 \mu\text{M}$) (**Figure 3**). Finally, as all the above assays employed cells transfected with substantially modified forms of the human GPR35 variants, we also conducted 'label-free' dynamic mass redistribution (DMR) experiments (Schröder et al., 2010, Deng et al., 2011, 2012) using HT-29 cells (**Figure 4**). Lodoxamide, bufrolin, zaprinast and cromolyn disodium all generated concentration-dependent modulation of the signal. Moreover, each ligand displayed both highly similar potencies and rank-order of potency as in the more artificial β -arrestin-2 interaction and receptor internalization assays, consistent with the effects of the ligands in HT-29 cells being mediated by GPR35 (**Figure 4A**). To further confirm that effects of lodoxamide reflected activation of GPR35, HT-29 cells were co-incubated with lodoxamide and various fixed concentrations of the human GPR35 specific (Jenkins et al., 2012) antagonist (Zhao et al., 2010) ML-145. This resulted in a parallel, surmountable and rightward shift of the concentration-response curve for lodoxamide, consistent with competitive interactions of the ligands with GPR35 (**Figure 4B**).

We (Jenkins et al., 2010, 2012, Neetoo-Isseljee et al., 2013) and others (Tanaguchi et al., 2006, Funke et al., 2013) have reported that many compounds first identified as ligands at human GPR35, including zaprinast, display markedly different potency and/or activity at rodent orthologs. We next examined, therefore, the activity of a variety of mast cell stabilizers at the rat ortholog of GPR35 in the BRET-based β -arrestin-2 interaction assay. Lodoxamide ($EC_{50} = 12.5 \pm 0.6 \text{ nM}$) was also a high potency agonist at rat GPR35 (**Figure 5**) and this was also true for bufrolin ($EC_{50} =$

MOL #89482

9.9 ± 0.4 nM) (**Figure 5**). As noted previously (Jenkins et al., 2010, 2011) zaprinast was substantially more potent ($EC_{50} = 98.4 \pm 3.7$ nM) at rat GPR35 (**Figure 5**) and amlexanox, although remaining a partial agonist compared to zaprinast, was some 500 fold more potent at the rat ortholog ($EC_{50} = 23.2 \pm 3.3$ nM) than at human GPR35a ($EC_{50} = 4.1 \pm 0.4$ μM) (**Figure 5**). As at the human receptor, tranilast and ketotifen fumarate displayed no significant activity (**data not shown**). However, in marked contrast to the human ortholog, pemirolast functioned as a high potency (94.8 ± 5.5 nM), full agonist at rat GPR35 (**Figure 5**), whilst doxantrazole also markedly gained potency and efficacy (**Figure 5**).

Given both that the novel ligands identified in these studies are negatively charged and that most are characterized by a strong planarity due to a series of fused rings (bufrolin, amlexanox, doxantrazole, pemirolast) we then performed a series of studies designed to define the mode of binding of the most potent ligands, i.e. lodoxamide and bufrolin and, although each of these ligands showed high potency at both human and rat GPR35, if there might be significant differences in the details of binding between the rat and human orthologs. As anticipated from previous work using zaprinast and kynurenic acid (Jenkins et al., 2011), replacement of Arg3.36 with Ala eliminated responsiveness to all of the ligands tested, confirming the importance of this residue (**not shown**). To extend these studies, initially we aligned the sequences of human GPR35a and rat GPR35 (**Figure 6A**) and, based on the fact that most GPR35 agonists are acids, acid bioisosteres or, even, di-acids with marked mirror image symmetry (**Figure 1**), we generated a series of reverse-swap mutations involving positively charged residues that vary between these species within regions

MOL #89482

of the TMDs and extracellular loops that recent comparative analysis of X-ray structures suggest may form parts of the general GPCR ligand binding pocket (Venkatakrisnan et al., 2013). Alteration in human GPR35a of Arg6.58 to Gln (Arg²⁴⁰Gln), as found in rat GPR35, resulted in modest reduction (1.5-6 fold) in potency of Iodoxamide, zaprinast and cromolyn disodium, but a substantially larger, 12 fold, reduction in potency for bufrolin (**Figure 6, Table 2**). The reverse mutation of Gln to Arg (Gln²³⁸Arg) in rat GPR35 resulted in no substantial changes in potency to these ligands (**Figure 6, Table 2**). More interestingly, alteration of Arg7.32 in human to the rat equivalent residue serine (Arg²⁵⁵Ser), as well as apparently reducing the overall efficacy response to ligands, resulted in a substantial decrease in potency to Iodoxamide (41 fold) without a corresponding effect on the potency of bufrolin (2 fold) but also with an increase in potency to both zaprinast (2 fold) and cromolyn disodium (4 fold) (**Figure 6, Table 2**). The reverse alteration of Ser7.32 to Arg (Ser²⁵³Arg) in rat GPR35 resulted in a small increase in potency for Iodoxamide (3 fold) without substantial effect on bufrolin and without changes in potency for zaprinast or cromolyn disodium (**Figure 6, Table 2**). Noticeably, however, as with the rat Gln6.58Arg mutation, this alteration also resulted in a marked increase in interactions between rat GPR35 and β -arrestin-2 in the absence of an agonist ligand, consistent with the introduction of a substantial level of constitutive activity (**Figure 6**). We next combined the alterations in sequence at positions 6.58 and 7.32 to generate human Gln6.58, Ser7.32 (Arg²⁴⁰Gln, Arg²⁵⁵Ser) GPR35a. This resulted in no alteration in potency of cromolyn disodium, a modest 3 fold reduction in potency to zaprinast but a virtual complete loss of function for Iodoxamide (at least 960 fold reduction) and also a large, 100 fold reduction in potency for bufrolin (**Figure 6,**

MOL #89482

Table 2). By contrast rat Arg6.58, Arg7.32 (Gln²³⁸Arg, Ser²⁵³Arg) GPR35 displayed equivalent potency for cromolyn disodium and bufrolin, a small decrease in potency for zaprinast and a similarly small increase in potency for lodoxamide. Most notably, however, rat Arg6.58, Arg7.32 GPR35 now displayed very high levels of ligand-independent constitutive activity (**Figure 6**). This feature was only observed at the rat ortholog; the reverse-swap mutations at human GPR35a had no significant effect on basal BRET signals (**Figure 6**).

The introduction of Arg instead of Leu at position 4.62 (Leu¹⁵³Arg) in human GPR35a enhanced the potency of zaprinast and cromolyn disodium, without significantly affecting the potency of lodoxamide or bufrolin (**Figure 7, Table 2**). By contrast, the corresponding switch from Arg4.62 to Leu (Arg¹⁵⁰Leu) in rat GPR35 resulted in a substantial reduction in potency for each of lodoxamide (46 fold) and cromolyn disodium (some 40 fold), with more limited effects for bufrolin (8 fold) and zaprinast (11 fold) (**Figure 7, Table 2**). Based on the markedly higher potency of both doxantrazole and pemirolast at rat GPR35 compared to human we also assessed the activity and potency of these ligands at the various species swap mutations described above with the largest effects being at the rat Arg4.62Leu GPR35 mutation with between 11- 30 fold reduction in potency (**Table 2**).

To attempt to provide a conceptual framework for these data we applied both further mutagenesis and homology modelling and ligand docking approaches to better understand the basis of ligand binding and species ortholog selectivity. Despite good overall structural similarity between the TMD helices of class A GPCRs crystallized to date (Venkatakrisnan et al., 2013), the extracellular side and, in particular, the

MOL #89482

extracellular loop 2 (ECL2), shows a very low conservation of both primary and tertiary structure (Mason et al., 2012, Wheatley et al., 2012). This is not surprising as parts of the ECL2 are frequently involved in ligand binding selectivity and potentially in initial ligand recognition, as are the extracellular faces of the helices. Moreover, human GPR35a possesses an arginine residue at position 164 that is lacking in rat, located two amino acids beyond the highly conserved Cys residue of ECL2 that is routinely involved in formation of a disulfide bridge. Mutation of this residue to the equivalent residue, serine, in rat produced a 60 fold reduction in potency for lodoxamide, but only a 4 fold reduction in potency for bufrolin (**Figure 7**), resulting in a reversal of the rank order of potency of these two ligands (**Figure 7**). The reciprocal mutation, to generate Ser¹⁶¹Arg rat GPR35 was without significant effect on the potency of either lodoxamide or bufrolin (**Figure 7**). Residue 4.60 is an arginine in both species (**Figure 6**). Mutation to methionine in either human or rat GPR35 resulted in reduction in potency of between 100-500 fold for both lodoxamide and zaprinast (**Figure 7, Table 2**) whilst the low potency of cromolyn disodium at wild type orthologs of GPR35 resulted in the loss of potency at Arg4.60Met being sufficient to prevent effective analysis of the data. By contrast, again at both species, this mutation had less effect on bufrolin, with loss of potency being only some 30 fold (**Figure 7, Table 2**).

The data appeared to favor a shared general binding site for lodoxamide and bufrolin, centered in the narrow space between TMD III and TMD VII, with the conserved Arg3.36 at its base and Arg4.60 providing the principal interaction residues for a negatively charged group from the ligands. Moreover, for lodoxamide at the

MOL #89482

human ortholog there appeared to be a potential, specific role for ECL2 and the mutational data indicated differences in detail of binding of lodoxamide and bufrolin with particular TMD arginine residues. Arg3.36 is potentially involved in an ionic interaction with Asp7.43 (**Figure 8**), that is likely disrupted by agonist binding. Lodoxamide and bufrolin are both characterized by the presence of two carboxyl groups (**Figure 1**). Modelling and docking studies, indeed, indicated a rather conserved location of binding within the two species but which varied in the detailed interactions with amino acids in the binding site (**Figure 8**). In human GPR35, which possesses arginine residues at positions 6.58 and 7.32 and a further arginine at position 164 in ECL2, these residues appear to be directly but differentially involved in binding these di-acidic groups (**Figure 8**). In agreement with data in **Table 2**, lodoxamide binding to human GPR35 reflects interaction of one of the carboxyl groups with both Arg3.36 and Arg4.60 while the other binds to Arg7.32 and Arg164 (**Figure 8A**). Consistent with such a model, a large reduction in potency for lodoxamide was observed when Arg7.32 was converted to serine whilst a gain of potency was observed for lodoxamide when serine7.32 in rat was altered to arginine (**Table 2**). Moreover, mutation of Arg164 resulted in a marked reduction in potency for lodoxamide (**Figure 7**). Bufrolin binds to human GPR35 in a similar pose as lodoxamide (**Figure 8B**), but based on the different structure of this ligand, Arg164 is less involved in binding, interacting only with a non-charged carbonyl oxygen, whilst alongside Arg3.36 at the base of the binding pocket and Arg4.60, which again binds one of carboxyl groups, Arg6.58 is the residue mainly involved in the interaction with

MOL #89482

the second carboxyl group (**Figure 8B**). The substantial reduction in potency of bufrolin at human Arg6.58Gln is consistent with this model, whereas potency of lodoxamide was less affected by this mutation. Interestingly, Arg7.32 in human GPR35 does not appear to be a substantial contributor to the binding of bufrolin and removal of this residue had a very modest effect on potency, whilst introduction of an arginine in this position in rat also did not alter potency significantly, but produced a modest increase in potency for lodoxamide. Rat GPR35 is characterized by the lack of the two arginines in TMD VI and TMD VII present in the human ortholog as well as that at position 161 (residue 164 in human ortholog, serine in rat) and by the presence of an arginine at position 4.62. As noted earlier mutation of this Arg to the equivalent human residue, Leu, strongly affect the potency of all ligands, particularly lodoxamide. In the rat GPR35 model Arg 4.62 acts as a surrogate of the human specific Arg164 and indeed this residue contributes more to the binding of lodoxamide binding than bufrolin (**Table 2**). Docking of lodoxamide and bufrolin to rat GPR35 predicts that Arg4.62 interacts with the second carboxyl group of these ligands, the first interacting with Arg3.36 and Arg4.60 (**Figure 8C, 8D**).

A prediction of these docking poses is that both the cyano group of lodoxamide and the propyl appendage of bufrolin point towards Val2.60 in human GPR35 (**Figures 8A, 8B**). Human GPR35 is markedly polymorphic, with a number of variations reported via the 1000 genomes sequencing project (1000 Genomes Project Consortium, 2010) that are predicted to be non-synonymous, therefore, to alter the amino acid sequence of the encoded polypeptide. One of these is Val⁷⁶Met i.e. at position 2.60. Although uncommon, with minor allele frequency = 0.014, we

MOL #89482

generated this variant and assessed responsiveness to lodoxamide and bufrolin in the BRET-based β -arrestin 2 interaction assay. Both ligands displayed substantially lower (13-15 fold) potency at the Met containing variant (**Figure 9, Table 3**). Moreover, a similar loss of potency to both zaprinast and cromolyn disodium was also observed at the Met containing variant (**Figure 9, Table 3**). The effect of the Val⁷⁶Met variant did not reflect issues with cell surface delivery: incorporation of an N-terminal FLAG epitope tag allowed ELISA-based detection of effective cell surface delivery and this was not different from the wild type receptor sequence (**Table 3**).

Six other distinct single amino acids variants, Ala²⁵Thr, Val²⁹Ile, Thr¹⁰⁸Met, Arg¹²⁵Ser, Thr²⁵³Met and Ser²⁹⁴Arg, of human GPR35a were generated, including those reported to have the highest minor allele frequency (Ser²⁹⁴Arg = 0.494, Thr¹⁰⁸Met = 0.161, Thr²⁵³Met = 0.058 and Arg¹²⁵Ser = 0.021) and those located within TMDs or extracellular segments of the receptor (Ala²⁵Thr, Val²⁹Ile). These were also assessed for effects on the potency of lodoxamide, zaprinast and cromolyn disodium using the GPR35a- β -arrestin-2 interaction assays. Unlike the Val⁷⁶Met variant, each of these was completely without effect on either the potency of the ligands or cell surface delivery (**Table 3**).

Discussion

Although the tryptophan metabolite kynurenic acid is able to activate GPR35 (Wang et al., 2006), the marked variation in potency between species orthologs and its very modest potency at the human receptor (Jenkins et al., 2011) has resulted in

MOL #89482

questions as to the physiological relevance of this ligand as (at least a human) GPR35 agonist (Milligan, 2011). This has also encouraged the search for other and more potent ligands to help define the functions of GPR35. This has included the suggestion that forms of lysophosphatidic acid might act as endogenous agonists (Oka et al., 2010). Among synthetic small molecule ligands, the anti-asthma and antiallergenic drugs cromolyn disodium (Jenkins et al., 2010, Yang et al., 2010) and nedocromil sodium (Yang et al., 2010) have been shown to have agonist activity at GPR35 and, although also of modest potency, this encouraged us to explore the possibility that other drugs with similar functional pharmacology might also be GPR35 agonists. Although this did not prove to be a generic feature, the fact that the function of both kynurenic acid and cromolyn disodium is lost following mutation of Arg3.36 (Jenkins et al., 2010) and that related receptors that have an arginine at this position also respond to small acidic ligands (Liu et al., 2009) led us to look more closely at this feature. The di-carboxyl containing antiallergenics lodoxamide and bufrolin were shown to be the most potent agonists of GPR35 yet identified, whilst amlexanox, a carboxylate-containing tricyclic anti-asthma drug was also a GPR35 agonist. Moreover, a number of other agonist ligands with anti-asthma/antiallergenic pharmacology, including doxantrazole and pemirolast, although lacking a carboxyl function, clearly contain an acid bioisostere related to the triazole structure present in the standard GPR35 surrogate agonist zaprinast. These ligands, although also active at GPR35, displayed marked differences in potency between the rat and human orthologs, a feature previously noted for zaprinast (Tanaguchi et al., 2006, Jenkins et al., 2010). Published literature indicates that certain GPR35 agonists, e.g. pamoate (Jenkins et al., 2010), 4-*{(Z)-[(2Z)-2-(2-fluorobenzylidene)-4-oxo-1,3-thiazolidin-5-*

MOL #89482

ylidene]methyl}benzoic acid (Neetoo-Isseljee et al., 2013) and various 8-benzamidochromen-4-one-2-carboxylic acids (Funke et al., 2013) are highly selective for the human ortholog whilst others, e.g. as shown here pemirolast and amlexanox, are highly selective for the rat ortholog. Although clearly speculation it may be interesting to consider if the inability to progress various antiallergics in the clinic may have a basis in this species selectivity. Based on the fact that each of pemirolast, zaprinast and amlexanox were markedly more potent in receptor- β -arrestin-2 interaction studies at the rat ortholog than at human GPR35, that the key residue Arg3.36 is conserved between species and because a number of GPR35 agonists, including lodoxamide and bufrolin, are di-acids we considered, therefore, the potential contribution to ligand recognition and potency of arginine residues in TMDs and near the top of the predicted TMD helix bundle that are not conserved between human and rat GPR35. This provided significant new insights. Furthermore, combinations of such mutations provided further insights. Although mutation of both Arg6.58 and Arg7.32 in human GPR35 has little effect on the potency of zaprinast it resulted in a greater than 900 fold reduction in potency for lodoxamide, a effect greater than predicted from either alteration alone. Results such as these encouraged us to apply homology modelling and computational ligand docking approaches to further explore the basis of ligand binding and species ortholog selectivity.

Despite strong structural similarity between the TMD helices of class A GPCRs crystallized to date, the extracellular side and, in particular, ECL2, show low conservation of both primary and tertiary structure (Wheatley et al., 2012, Venkatakrisnan et al., 2013). This is not surprising as parts of the ECL2 are

MOL #89482

frequently involved in ligand binding and potentially in initial ligand recognition, as are elements of the extracellular face of the helices. Human and rat GPR35 (71% sequence identity, 81% in the transmembrane helices) differ in both sequence and length of ECL2, potentially the most relevant differences being an arginine in rat GPR35 at position 4.62 (leucine in human), and a serine (arginine in human) and a glutamine (missing in human) that are located respectively two and four residues after the cysteine involved in the conserved disulfide bridge between ECL2 and TMD III. These species variations strongly affect the residues of ECL2 involved in ligand binding. Such differences, however, pose substantial challenges for homology modelling and ligand docking studies.

All GPR35 agonist ligands are negatively charged or possess acid bioisosteres and are frequently characterized by a strong planarity, either due to a series of fused rings (bufrolin, amlexanox, doxantrazole, pemirolast) or induced by intra-molecular hydrogen bonds, as in zaprinast. In contrast, lodoxamide contains a single aromatic ring. The results of the mutational studies generally suggested a common binding site, centered between TMD III and TMD VII, with the core conserved Arg3.36, which forms an ionic interaction with Asp 7.43 in the basal state, at its base providing, together with Arg4.60, the principal interaction residues for a negatively charged group of the ligands. Lodoxamide and bufrolin are characterized by the presence of two carboxyl groups and, unusually for GPR35 ligands, are highly potent at both the human and rat orthologs. Although they bind in similar regions in different species orthologs distinct, species-specific arginines, all at the extracellular side of the binding cavity are involved in binding the second carboxyl group of both lodoxamide and brufolin.

MOL #89482

A prediction of the docking pose in human GPR35 illustrated is that the cyano group of lodoxamide points towards Val2.60. Moreover, the propyl appendage of bufrolin is also predicted to orientate towards this residue. It is of particular interest, therefore, that Val2.60Met was the only human non-synonymous SNP variant we assessed that modified the potency of these GPR35 agonists. It is therefore reasonable, based on this model and docking pose, to suggest that steric hindrance may be responsible for the potency decrease observed in the human GPR35 Val2.60Met variant. The loss of potency for both zaprinast and cromolyn disodium also hints at a similar general binding location as for lodoxamide and bufrolin and, as shown previously for zaprinast and cromolyn disodium (Jenkins et al., 2011), with all these ligands being ‘orthosteric’ with respect to one another. However, as zaprinast and cromolyn disodium are far less potent than lodoxamide and bufrolin at the human receptor this is challenging to model directly and there must be substantial differences in detail given the modest effect on the potency of these ligands of a number of the mutants we characterized.

There is considerable interest in the idea that non-synonymous SNP variation in the open reading frame of receptor sequences may help define the basis of distinct responsiveness to drugs and be important for the continuing efforts to personalise therapy and treatment. GPR35 is markedly polymorphic in the open reading frame but accumulating evidence suggests that many of these are infrequent alleles. However, as a number of the reported variants in human GPR35 are located either within TMDs or at the interface of the helix bundle and the connecting extracellular loops we also explored the pharmacology of a number of other variants, including Thr¹⁰⁸Met, located in transmembrane domain III and Thr²⁵³Met located within extracellular loop

MOL #89482

III as these both are reported to occur with significant allelic frequency. However, despite rs3749171, a SNP associated in genome-wide association analyses as a risk locus for ulcerative colitis (Ellinghaus et al., 2013) and IBD (Jostins et al., 2012), encompassing the GPR35 locus, at least in the receptor- β -arrestin-2 interaction assays employed, neither of these variations had any detectable effect on ligand pharmacology.

In conclusion we report the identification of antiallergic compounds with low nM potency for human GPR35. In contrast to the marked variation in potency of many previously described agonists of GPR35 between human and rodent orthologs, both lodoxamide and bufrolin are also highly potent at rat GPR35 with a predicted mode of binding similar to that of human GPCR35a. Remarkably, the ligand docking studies on these ligands suggested that an uncommon, non-synonymous variant of this receptor in the human population might display marked variation in ligand potency and this was confirmed experimentally to be correct.

MOL #89482

Acknowledgements

We thank Dr Ed McIver and Dr Debbie Taylor, Medical Research Council Technology, London UK for provision of Iodoxamide and Dr. John Souness, Sanofi, for insight and helpful discussions. The DMR assays were conducted at the laboratories of Medical Research Council Technology under the guidance of Craig Southern and Zaynab Neetoo-Isseljee.

Authorship Contributions

Participated in research design; MacKenzie, Kent, Hudson, Nicklin, Charlton, Milligan

Conducted experiments; MacKenzie, Caltabiano, Jenkins, McCallum, Hudson, Fawcett, Lane

Contributed new reagents or analytic tools; Kent, Charlton

Performed data analysis; Mackenzie, Caltabiano, Hudson, Kent, Milligan

Wrote or contributed to writing of manuscript, MacKenzie, Milligan

MOL #89482

References

1000 Genomes Project Consortium, Abecasis GR, Altshuler D, Auton A, Brooks LD, Durbin RM, Gibbs RA, Hurles ME, and McVean GA (2010) A map of human genome variation from population-scale sequencing. *Nature* **467**:1061-1073.

Ballesteros JA, and Weinstein H (1995) Integrated methods for modeling G-Protein Coupled Receptors. *Methods Neurosci* 366-428.

Cordomí A, Caltabiano G, and Pardo L (2012) Membrane protein simulations using AMBER force field and Berger lipid parameters. *J Chem Theory Comput* **8**: 948-958.

Deng H, Hu H, He M, Hu J, Niu W, Ferrie AM, and Fang Y (2011) Discovery of 2-(4-methylfuran-2(5H)-ylidene)malononitrile and thieno[3,2-b]thiophene-2-carboxylic acid derivatives as G protein-coupled receptor 35 (GPR35) agonists. *J Med Chem* **54**:7385-7396.

Deng H, Hu H, Ling S, Ferrie AM, and Fang Y (2012) Discovery of natural phenols as G protein-coupled receptor-35 (GPR35) agonists. *ACS Med Chem Lett* **3**:165-169.

Ellinghaus D, Folseraas T, Holm K, Ellinghaus E, Melum E, Balschun T, Laerdahl JK, Shiryaev A, Gotthardt DN, Weismüller TJ, Schramm C, Wittig M, Bergquist A, Björnsson E, Marschall HU, Vatn M, Teufel A, Rust C, Gieger C, Wichmann HE, Runz H, Sterneck M, Rupp C, Braun F, Weersma RK, Wijmenga C, Ponsioen CY, Mathew CG, Rutgeerts P, Vermeire S, Schrumpf E, Hov JR, Manns MP, Boberg KM,

MOL #89482

Schreiber S, Franke A, and Karlsen TH (2013) Genome-wide association analysis in sclerosing cholangitis and ulcerative colitis identifies risk loci at GPR35 and TCF4.

Hepatology **58**:1074-1083.

Funke M, Thimm D, Schiedel AC, Müller CE (2013) 8-Benzamidochromen-4-one-2-carboxylic acids: Potent and selective agonists for the orphan G Protein-Coupled Receptor GPR35. *J Med Chem* **56**:5182-5197.

Hess B, Kutzner C, van der Spoel D, and Lindahl, E. (2008) GROMACS 4: Algorithms for highly efficient, load-balanced, and scalable molecular simulation. *J. Chem. Theory Comput* **4**: 435-447.

Jenkins L, Alvarez-Curto E, Campbell K, de Munnik S, Canals M, Schlyer S, and Milligan G (2011) Agonist activation of the G protein-coupled receptor GPR35 involves transmembrane domain III and is transduced via Galpha and beta-arrestin-2. *Br J Pharmacol* **162**: 733-748.

Jenkins L, Brea J, Smith NJ, Hudson BD, Reilly G, Bryant NJ, Castro M, Loza MI, and Milligan G (2010) Identification of novel species-selective agonists of the G-protein-coupled receptor GPR35 that promote recruitment of beta-arrestin-2 and activate Galpha13. *Biochem J* **432**: 451-459.

Jenkins L, Harries N, Lappin JE, MacKenzie AE, Neetoo-Isseljee Z, Souther, C, McIver E., Nicklin SA, Taylor DL, and Milligan G (2012) Antagonists of GPR35

MOL #89482

display high species ortholog selectivity and varying modes of action. *J Pharmacol*

Exp Ther **343**: 683-695

Jostins L, Ripke S, Weersma RK, Duerr RH, McGovern DP, Hui KY, Lee JC, Schumm LP, Sharma Y, Anderson CA, Essers J, Mitrovic M, Ning K, Cleynen I, Theatre E, Spain SL, Raychaudhuri S, Goyette P, Wei Z, Abraham C, Achkar JP, Ahmad T, Amininejad L, Ananthakrishnan AN, Andersen V, Andrews JM, Baidoo L, Balschun T, Bampton PA, Bitton A, Boucher G, Brand S, Büning C, Cohain A, Cichon S, D'Amato M, De Jong D, Devaney KL, Dubinsky M, Edwards C, Ellinghaus D, Ferguson LR, Franchimont D, Fransen K, Gearry R, Georges M, Gieger C, Glas J, Haritunians T, Hart A, Hawkey C, Hedl M, Hu X, Karlsen TH, Kupcinkas L, Kugathasan S, Latiano A, Laukens D, Lawrance IC, Lees CW, Louis E, Mahy G, Mansfield J, Morgan AR, Mowat C, Newman W, Palmieri O, Ponsioen CY, Potocnik U, Prescott NJ, Regueiro M, Rotter JI, Russell RK, Sanderson JD, Sans M, Satsangi J, Schreiber S, Simms LA, Sventoraityte J, Targan SR, Taylor KD, Tremelling M, Verspaget HW, De Vos M, Wijmenga C, Wilson DC, Winkelmann J, Xavier RJ, Zeissig S, Zhang B, Zhang CK, and Zhao H: International IBD Genetics Consortium (IIBDGC), Silverberg MS, Annese V, Hakonarson H, Brant SR, Radford-Smith G, Mathew CG, Rioux JD, Schadt EE, Daly MJ, Franke A, Parkes M, Vermeire S, Barrett JC, and Cho JH (2012) Host-microbe interactions have shaped the genetic architecture of inflammatory bowel disease. *Nature* **491**:119-124.

Liu C, Wu J, Zhu J, Kuei C, Yu J, Shelton J, Sutton SW, Li X, Yun SJ, Mirzadegan T, Mazur C, Kamme F, and Lovenberg TW (2009) Lactate inhibits lipolysis in fat cells

MOL #89482

through activation of an orphan G-protein-coupled receptor, GPR81. *J Biol Chem* **284**:2811-2822.

Lumb EM, McHardy GJ, and Kay AB (1979) The orally administered anti-allergic agent, sodium nivimedone (BRL 10833); efficacy in bronchial asthma and effects on IgE, complement and eosinophils. *Br J Clin Pharmacol* **8**:65-74.

MacKenzie AE, Lappin JE, Taylor DL, Nicklin SA and Milligan G (2011) GPR35 as a novel therapeutic target. *Front Endocrin Molecular and Structural Endocrinology* **2**: 68.

Martí-Renom MA, Stuart AC, Fiser A, Sánchez R, Melo F, and Sali A (2000) Comparative protein structure modeling of genes and genomes. *Annu Rev Biophys Biomol Struct* **29**:291-325.

Mason JS, Bortolato A, Congreve M, and Marshall FH (2012) New insights from structural biology into the druggability of G protein-coupled receptors. *Trends Pharmacol Sci* **33**:249-260.

Milligan G (2011) Orthologue selectivity and ligand bias: translating the pharmacology of GPR35. *Trends Pharmacol Sci* **32**:317-325.

MOL #89482

Neetoo-Isseljee Z, MacKenzie AE, Southern C, Jerman J, McIver EG, Harries N, Taylor DL, and Milligan G (2013) High throughput identification and characterization of novel, species-selective GPR35 agonists. *J Pharmacol Exp Ther* **344**:568-578.

Oka S, Ota R, Shima M, Yamashita A, and Sugiura T (2010) GPR35 is a novel lysophosphatidic acid receptor. *Biochem Biophys Res Commun* **395**:232-237.

Okumura S, Baba H, Kumada T, Nanmoku K, Nakajima H, Nakane Y, Hioki K, and Ikenaka K (2004) Cloning of a G-protein-coupled receptor that shows an activity to transform NIH3T3 cells and is expressed in gastric cancer cells. *Cancer Sci* **95**:131-135.

Salon JA, Lodowski DT, and Palczewski K (2011) The significance of G protein-coupled receptor crystallography for drug discovery. *Pharmacol Rev* **63**: 901-937.

Schröder R, Janssen N, Schmidt J, Kebig A, Merten N, Hennen S, Müller A, Blättermann S, Mohr-Andrä M, Zahn S, Wenzel J, Smith NJ, Gomeza J, Drewke C, Milligan G, Mohr K, and Kostenis E (2010) Deconvolution of complex G protein-coupled receptor signaling in live cells using dynamic mass redistribution measurements. *Nat Biotechnol* **28**:943-949.

Schrodinger L (2012) The PyMOL Molecular Graphics System, Version 1.5r3,

Southern C, Cook JM, Neetoo-Isseljee Z, Taylor DL, Kettleborough CA, Merritt A, Bassoni DL, Raab WJ, Quinn E, Wehrman TS, Davenport AP, Brown AJ, Green A,

MOL #89482

Wigglesworth MJ, and Rees S (2013) Screening β -arrestin recruitment for the identification of natural ligands for orphan G-protein-coupled receptors. *J Biomol Screen* **18**:599-609.

Sun YV, Bielak LF, Peyser PA, Turner ST, Sheedy PF 2nd, Boerwinkle E and Kardia SL (2008) Application of machine learning algorithms to predict coronary artery calcification with a sibship-based design. *Genet Epidemiol* **32**:350-360.

Taniguchi Y, Tonai-Kachi H, and Shinjo K (2006) Zaprinast, a well-known cyclic guanosine monophosphate-specific phosphodiesterase inhibitor, is an agonist for GPR35. *FEBS Lett* **580**:5003-5008.

Venkatakrishnan AJ, Deupi, X., Lebon, G., Tate, CG, Schertler GF and Babu, MM (2013) Molecular signatures of G-protein-coupled receptors. *Nature* **494**:185-194.

Wang J, Simonavicius N, Wu X, Swaminath G, Reagan J, Tian H, and Ling L (2006) Kynurenic acid as a ligand for orphan G protein-coupled receptor GPR35. *J Biol Chem* **281**:22021-22028.

Wheatley M, Wootten D, Conner MT, Simms J, Kendrick R, Logan RT, Poyner DR, and Barwell J (2012) Lifting the lid on GPCRs: the role of extracellular loops. *Br J Pharmacol* **165**:1688-1703.

MOL #89482

Yang Y, Lu JY, Wu X, Summer S, Whoriskey J, Saris C, and Reagan JD (2010) G-protein-coupled receptor 35 is a target of the asthma drugs cromolyn disodium and nedocromil sodium. *Pharmacology* **86**:1-5.

Zhang C, Srinivasan Y, Arlow DH, Fung JJ, Palmer D, Zheng Y, Green H, Pandey, A, Dror RO, Shaw DE, Weis WI, Coughlin SR, and Kobilka BK (2012) High-resolution crystal structure of human protease-activated receptor 1. *Nature* **492**: 387-392.

Zhao P, Sharir H, Kapur A, Cowan A, Geller EB, Adler MW, Seltzman HH, Reggio PH, Heynen-Genel S, Sauer M, Chung TD, Bai Y, Chen W, Caron MG, Barak LS, and Abood ME (2010) Targeting of the orphan receptor GPR35 by pamoic acid: a potent activator of extracellular signal-regulated kinase and beta-arrestin-2 with antinociceptive activity. *Mol Pharmacol* **78**: 560-568.

Footnotes

AEM thanks the Biotechnology and Biosciences Research Council and Medical Research Council Technology for an industrial CASE studentship and JEM thanks British Heart Foundation for studentship support. GC was in receipt of a "José Castillejo 2012" fellowship, provided by the Spanish Ministerio de Educación, Cultura y Deporte, Programa Nacional de Movilidad de Recursos Humanos del Plan Nacional de I-D+i 2008-2011.

MOL #89482

Legends for Figures

Figure 1 Structures of key GPR35 ligands

The structures of key ligands used in the studies are shown.

Figure 2 Some, but not all, antiallergenics are GPR35 agonists

The ability of a range of compounds that have effectiveness as antiallergenics and mast cell stabilizers, including lodoxamide (**filled circles**), bufrolin (**open squares**), amlexanox (**filled triangles**), doxantrazole (**open diamonds**), pemirolast (**inverted filled triangles**) and cromolyn disodium (**open circles**), to promote interactions between human GPR35a (**A**) or human GPR35b (**B**) and β -arrestin-2 was compared to the prototypic GPR35 agonist zaprinast (**filled diamonds**) in BRET-based assays. As noted in results, the absolute signals obtained using GPR35b were substantially lower than when using GPR35a.

Figure 3 High content analysis of internalization of human GPR35a confirms agonism of certain antiallergenics at this receptor

The capacity of varying concentrations of lodoxamide (**filled circles**), bufrolin (**open squares**), zaprinast (**filled diamonds**) or cromolyn disodium (**open circles**) to promote internalization of human GPR35a-eYFP was assayed and quantified via high content analysis as number of endocytic recycling compartments (ERC) per cell (**A**). (**B**) Representative images of the cellular distribution of human FLAG-GPR35a-eYFP

MOL #89482

at the times indicated following addition of maximally effective concentrations of lodoxamide (5 μ M), bufrolin (100 nM), zaprinast (50 μ M) and cromolyn disodium (100 μ M) are displayed.

Figure 4 Dynamic Mass Redistribution studies indicate that ligand effects in HT29 cells are mediated via GPR35.

The capacity of varying concentrations of lodoxamide (**filled circles**), bufrolin (**open squares**), zaprinast (**filled diamonds**) and cromolyn disodium (**open circles**) to modulate DMR signals in HT29 cells is shown (**A**). (**B**). Effects of defined concentrations of the human GPR35 specific antagonist ML-145 on the agonist effects of lodoxamide are shown.

Figure 5 Lodoxamide and bufrolin are high potency agonists at both human and rat GPR35 whereas other ligands display substantial species ortholog selectivity

The ability of varying concentrations of lodoxamide (**A**), bufrolin (**B**), zaprinast (**C**) amlexanox (**D**), doxantrazole (**E**) and pemirolast (**F**) to promote interactions between β -arrestin-2 and either human GPR35a or rat GPR35 in BRET-based assays is shown.

Figure 6 Swapping non-conserved arginine residues between human and rat GPR35a influences ligand potency

Alignment of the sequences of human GPR35a and rat GPR35. Key residues that vary between the two orthologs that were swapped between species or otherwise modified

MOL #89482

are highlighted, as are the conserved arginine at position 3.36 that acts as a key ligand binding contact in both species and the aspartate at position 7.43, predicted to form an ionic interaction with arginine 3.36 in the absence of agonist. **B**. Mutations altered the basal, ligand independent activity at rat GPR35 but not at human GPR35a.

Significantly different from wild type at $p < 0.05$ *, $p < 0.01$ **, or $p < 0.001$ ***. The ability of lodoxamide (**C**), bufrolin (**D**), zaprinast (**E**) and cromolyn disodium (**F**) to promote interactions between human GPR35a (**left hand side**) and rat GPR35 (**right hand side**) are shown for wild type (**WT**) and ortholog residue swaps at positions 6.58, 7.32 and 6.58 plus 7.32.

Figure 7 Alterations of further conserved and non-conserved residues also affect ligand potency at GPR35

Residue 4.60 is an arginine in both human and rat orthologs of GPR35 and was converted to methionine, whilst residue 4.62, leucine in human but arginine in rat, was swapped between species. Arginine 164 in ECL2 of human GPR35a was converted to serine whilst the equivalent residue, 161 in rat GPR35, was altered to arginine. These mutants were then compared to the wild type sequences in BRET-based GPR35 β -arrestin-2 interaction studies to explore effects on the potency of lodoxamide (**A**), bufrolin (**B**), zaprinast (**C**) and cromolyn disodium (**D**). Human GPR35a (**left hand side**), rat GPR35 (**right hand side**)

MOL #89482

Figure 8 Homology modelling and ligand docking studies of human and rat GPR35a

Potential modes of binding of lodoxamide (**A, C**) and bufrolin (**B, D**) to human GPR35a (**A, B**) and rat GPR35 (**C, D**) are shown. These are consistent with mutational data shown in Figures 6 and 7 and quantified in Table 2.

Figure 9 The polymorphic variant Val⁷⁶Met reduces potency of a series of ligands at human GPR35a

The potency of lodoxamide (**A**), bufrolin (**B**), zaprinast (**C**) and cromolyn disodium (**D**) were compared between human Val⁷⁶ GPR35a and Met⁷⁶ GPR35a using the BRET-based β -arrestin-2 interaction assay. In each case data are presented as a % of the maximal effect of zaprinast at the appropriate variant.

MOL #89482

Table 1 A number of anti-asthma and antiallergenics act as potent agonists of human GPR35a

Compound	EC₅₀ (nM) (mean +/- SEM)
Nedocromil sodium	970 ± 87.0
Cromolyn disodium	2980 ± 127
Bufrolin	2.93 ± 0.71
Lodoxamide	1.61 ± 0.42
Nivimedone sodium	1930 ± 348
Tranilast	No response

PathHunter™ human GPR35a-β-arrestin-2 interaction assays were performed using a CHO-K1 cell line stably expressing human GPR35 and β-arrestin-2. Data are derived from 3 independent experiments.

MOL #89482

Table 2 Effects of arginine swap mutations on ligand pharmacology at human and rat GPR35

Human GPR35a pEC₅₀ values and ΔpEC₅₀ compared with wild type

Ligand	Wild Type	Arg ¹⁶⁴ Ser		Arg 4.60 Met		Leu 4.62 Arg		Arg 6.58 Gln		Arg 7.32 Ser		Arg 6.58 Glu, Arg 7.32 Ser	
Zaprinast	5.59 ± 0.01	5.45 ± 0.08	-0.14	<4	<-1.59	6.13 ± 0.04***	+0.54	5.11 ± 0.05***	-0.48	5.99 ± 0.09***	+0.4	5.08 ± 0.05***	-0.51
Lodoxamide	8.44 ± 0.02	6.65 ± 0.09***	-1.79	5.88 ± 0.04***	-2.56	8.63 ± 0.09	+0.19	8.19 ± 0.09	-0.25	6.83 ± 0.01***	-1.61	<4	<-4.44
Bufrolin	7.90 ± 0.04	7.36 ± 0.001*	-0.54	6.28 ± 0.05***	-1.62	8.18 ± 0.05	+0.28	6.82 ± 0.09***	-1.08	7.61 ± 0.1	-0.29	5.88 ± 0.23***	-2.02
Cromolyn	5.20 ± 0.03	4.3 ± 0.13***	-0.9	<4	<-1.20	5.72 ± 0.04***	+0.52	5.05 ± 0.04	-0.15	5.95 ± 0.15***	+0.75	5.23 ± 0.08	+0.03
Amlexanox	5.39 ± 0.06	5.28 ± 0.04	-0.11	4.48 ± 0.09***	-0.91	5.83 ± 0.09	+0.44	5.54 ± 0.11	+0.15	5.86 ± 0.15*	+0.47	5.74 ± 0.11	+0.35
Doxantrazole	5.47 ± 0.07	5.27 ± 0.01	-0.2	5.11 ± 0.06	-0.36	5.69 ± 0.06	+0.22	5.09 ± 0.12	-0.38	5.87 ± 0.17	+0.4	5.03 ± 0.11	-0.44
Pemiroloast	<4	<4	N/A	<4	N/A	<4	N/A	<4	N/A	<4	N/A	<4	N/A

Rat GPR35 pEC₅₀ values and ΔpEC₅₀ compared with wild type

Ligand	Wild Type	Ser ¹⁶¹ Arg		Arg 4.60 Met		Arg 4.62 Leu		Gln 6.58 Arg		Ser 7.32 Arg		Glu 6.58 Arg, Ser 7.32 Arg	
Zaprinast	7.01 ± 0.02	6.07 ± 0.02***	-0.94	5.03 ± 0.08***	-1.98	5.96 ± 0.04***	-1.05	6.97 ± 0.08	-0.04	7.03 ± 0.06	+0.02	6.77 ± 0.2	-0.24
Lodoxamide	7.90 ± 0.02	7.47 ± 0.002**	-0.43	5.18 ± 0.13***	-2.72	6.24 ± 0.07***	-1.66	8.09 ± 0.08	+0.19	8.25 ± 0.08**	+0.35	8.15 ± 0.2*	+0.25
Bufrolin	8.00 ± 0.02	8.08 ± 0.007	+0.08	7.25 ± 0.26*	-0.75	7.11 ± 0.06**	-0.89	8.16 ± 0.1	+0.16	8.1 ± 0.1	+0.1	7.88 ± 0.28	-0.12
Cromolyn	5.42 ± 0.03	4.32 ± 0.12***	-1.1	<4	<-1.42	<4	<-1.42	5.33 ± 0.06	-0.09	5.57 ± 0.10	+0.15	5.48 ± 0.34	+0.06
Amlexanox	7.63 ± 0.07	5.86 ± 0.05***	-1.77	5.66 ± 0.27***	-1.97	6.93 ± 0.06**	-0.7	7.50 ± 0.12	-0.13	7.59 ± 0.15	-0.04	7.23 ± 0.18	-0.4
Doxantrazole	6.51 ± 0.02	5.35 ± 0.09***	-1.16	5.28 ± 0.25***	-1.23	4.98 ± 0.16***	-1.53	6.37 ± 0.12	-0.14	7.15 ± 0.13**	+0.64	6.70 ± 0.47	+0.19
Pemiroloast	7.02 ± 0.03	5.78 ± 0.08***	-1.24	5.05 ± 0.46***	-1.97	5.97 ± 0.04***	-1.05	6.86 ± 0.09	-0.16	7.49 ± 0.12**	+0.47	6.64 ± 0.29*	-0.38

All studies employed the BRET-based GPR35-β-arrestin 2 interaction assay. pEC₅₀ significantly different from corresponding wild type at p < 0.05 *, p < 0.01**, or p < 0.001 ***. Potency estimates of < 4 reflect lack of adequate data fit. N/A; not applicable, as pemiroloast lacked potency at wild type human GPR35a.

MOL #89482

Table 3 Lack of effect of most polymorphic variants of human GPR35a on ligand potency

Variant	Expression^a	Lodoxamide EC₅₀ (nM)	Zaprinast EC₅₀ (μM)	Cromolyn EC₅₀ (μM)
Ala²⁵Thr	0.97 ± 0.13	3.70 ± 1.76	1.84 ± 0.66	2.94 ± 0.48
Val²⁹Ile	1.27 ± 0.15	3.58 ± 1.67	1.70 ± 0.49	3.70 ± 1.72
Val⁷⁶Met	1.06 ± 0.08	33.38 ± 16.85*	16.37 ± 5.84*	20.26 ± 4.86*
Thr¹⁰⁸Met	0.67 ± 0.14	6.49 ± 3.80	3.12 ± 1.07	5.36 ± 1.83
Arg¹²⁵Ser	1.32 ± 0.16	5.25 ± 2.80	1.55 ± 0.62	3.73 ± 1.43
Thr²⁵³Met	0.63 ± 0.18	2.50 ± 0.95	1.60 ± 0.75	1.86 ± 0.74
Ser²⁹⁴Arg	1.48 ± 0.51	3.07 ± 1.46	1.14 ± 0.48	1.95 ± 0.19
Wild type	1.00 ± 0.23	3.97 ± 1.77	2.29 ± 0.79	2.98 ± 1.27

a Expression as fold relative to wild type

The possible effect of non-synonymous SNP variation in human GPR35a on ligand potency was assessed for a number of previously reported examples (1000 Genomes Project Consortium, 2010). In each case the minor allele amino acid (listed second) was introduced into otherwise wild type human GPR35a and ligand potency then assessed in PathHunter™ human GPR35a-β-arrestin-2 interaction assays as in Table 1. Only in the case of Val⁷⁶Met was a significant (*p < 0.05) alteration in potency recorded.

Figure 1

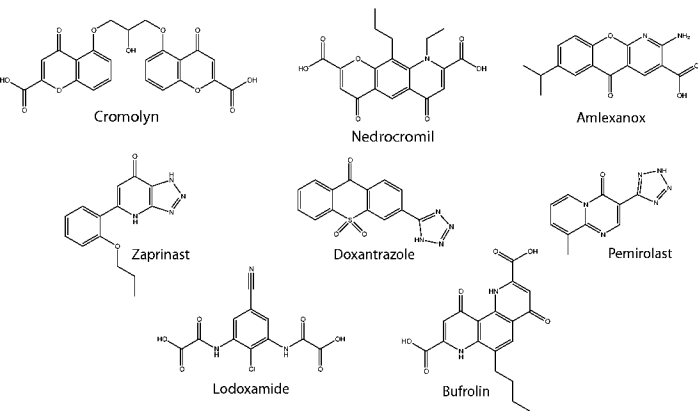


Figure 2

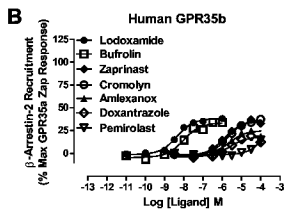
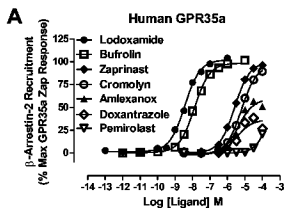
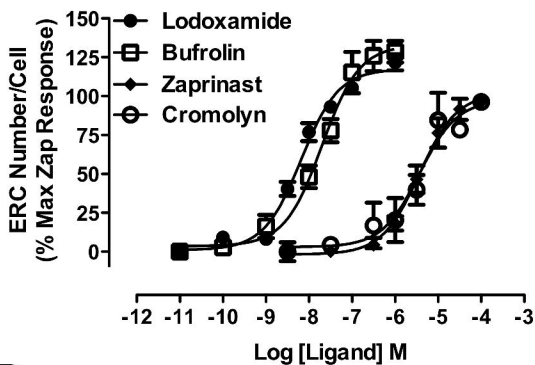


Figure 3

A



B

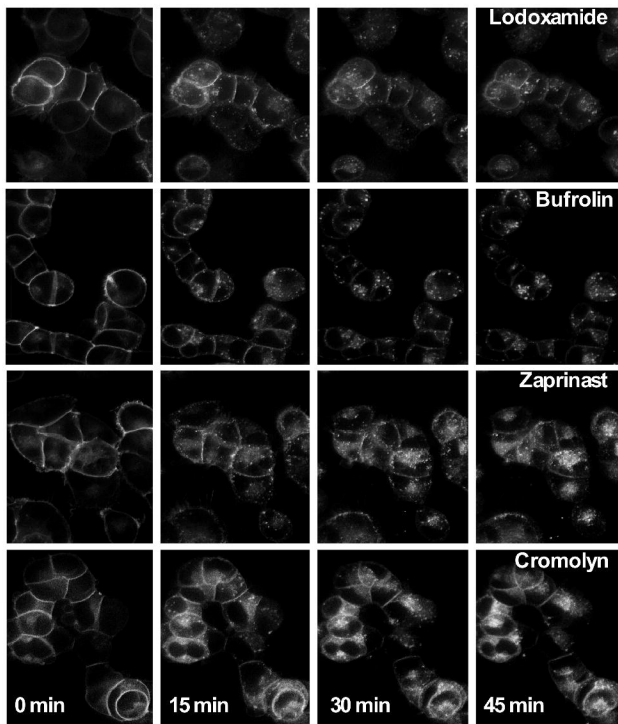


Figure 4

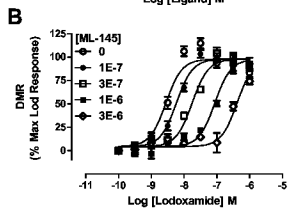
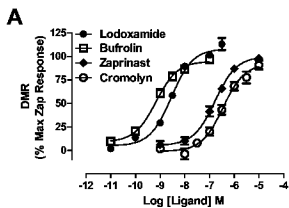


Figure 5

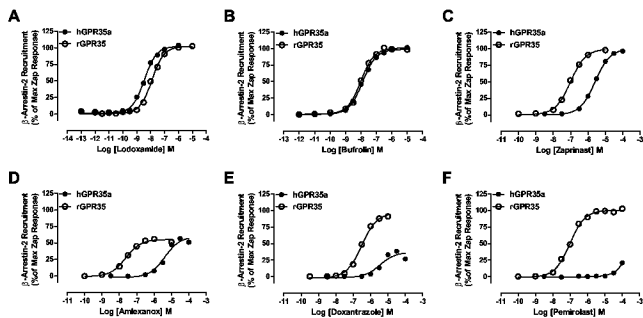


Figure 7

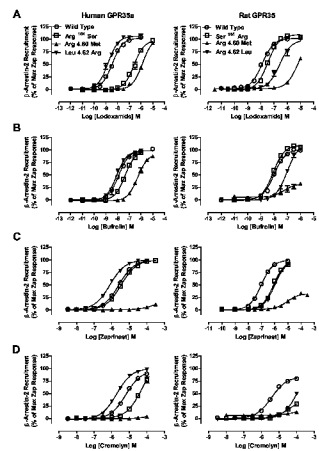


Figure 8

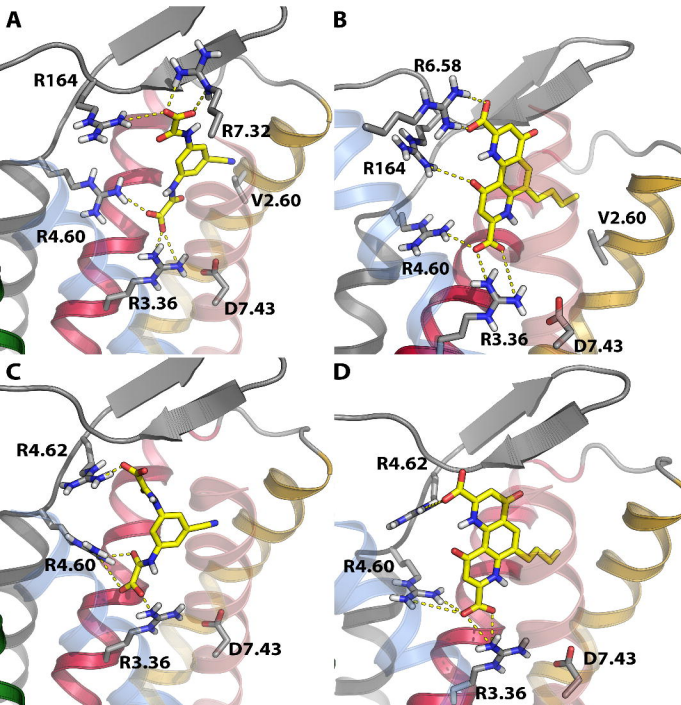


Figure 9

